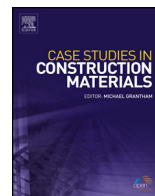




ELSEVIER

Contents lists available at ScienceDirect

## Case Studies in Construction Materials

journal homepage: [www.elsevier.com/locate/cscm](http://www.elsevier.com/locate/cscm)

# Performance of slab-column connections of flat slabs strengthened with carbon fiber reinforced polymers

M.A.L. Silva<sup>a,\*</sup>, J.C.P.H. Gamage<sup>a</sup>, S. Fawzia<sup>b</sup><sup>a</sup> Department of Civil Engineering, University of Moratuwa, Sri Lanka<sup>b</sup> Civil Engineering, Queensland University of Technology, Australia

## ARTICLE INFO

## Article history:

Received 16 May 2019

Received in revised form 29 July 2019

Accepted 15 August 2019

## Keywords:

CFRP

External strengthening

Numerical modeling

Punching shear enhancement

Slab/column interface

## ABSTRACT

Retrofitting of slab-column connections has become a crucial concern as they are highly vulnerable to fail in punching shear failure. External strengthening is practically feasible rather than the post-installation of shear reinforcement in deteriorated slab-column connections. Hence, the behavior of medium scale slab-column junctions strengthened with alternative arrangements of Carbon Fiber Reinforced Polymer (CFRP) was studied. Numerical models were also developed to analyze bond behavior. The model predicted performances are in good agreement with the test results. The maximum average punching shear enhancement of 46% was observed from the specimens with CFRP plates attached to the tension face of the specimens with steel end anchors.

© 2019 Published by Elsevier Ltd. This is an open access article under the CC BY-NC-ND license (<http://creativecommons.org/licenses/by-nc-nd/4.0/>).

## 1. Introduction

Punching shear strength of a slab-column connection becomes critical due to several causes such as change of building use, need of installing new services which requires openings in the slabs, corrosion of reinforcement and, construction or design errors. These issues may induce the need of retrofitting of the slab-column connections within the service life of a structure. Carbon Fiber Reinforced Polymer (CFRP) materials can be successfully used to enhance the flexure and shear performance of slab-column connections [1]. Strengthening of reinforced concrete flat slabs using CFRP can be done in two methods; External strengthening [2–4] and internal strengthening [6]. Depending on the strengthening requirement, a suitable strengthening method has to be selected and implemented. Post-installation of shear reinforcements falls into internal strengthening category and external attaching of CFRP using epoxy adhesive falls into external strengthening category. Since the slab-column connections are vulnerable to punching shear failure, the post-installation of shear reinforcements in the shear critical area could damage the shear critical area furthermore, if not properly repaired [6]. In order to overcome this problem, the external application of CFRP can be introduced as a non-damaging retrofitting method. The increase in flexural reinforcement ratio increases the punching shear capacity [2,7] by delaying the formation of shear cracks [5]. The provision of end anchorages to externally attached CFRP could increase the load carrying capacity of slabs furthermore [7–9]. According to the research studies conducted, the post-installation of CFRP shear dowels or CFRP studs in the shear critical area indicated a performance enhancement in the range of 17%–97% [10,11]. The research studies conducted using pre-installed shear reinforcements had shown a maximum shear capacity increment of 100% [12]. This may not be achieved in retrofitting approaches of flat slabs using post-installation of CFRP shear reinforcements if a suitable epoxy grout

\* Corresponding author.

E-mail address: [anulaksilva@gmail.com](mailto:anulaksilva@gmail.com) (M.A.L. Silva).

refilling material is not used to fill the drilled hole area to create a perfect bond between the shear reinforcement and concrete.

External strengthening near the column face using CFRP to enhance the punching shear capacity is an alternative solution as a non-drilling retrofitting method [2,4]. Studies conducted on externally strengthened slabs indicated a strength enhancement in the range of 39%–56% [13]. In general, further damaging of a degraded slab near the punching shear critical area to insert shear reinforcements is not a practically favorable solution in many situations. Therefore, this research study focuses on identifying the key factors of an external CFRP strengthening scheme which can govern the performance of a flat slab-column connection.

## 2. Test program

### 2.1. Overview

The behavior of slab-column connections retrofitted with alternative arrangements of externally attached CFRP was studied. Ten flat slab specimens of size 1200 mm × 1200 mm × 100 mm (Fig. 1) were prepared with a center stub column connected monolithically to the slab. Two specimens were kept as non-strengthened control specimens and others were strengthened against punching shear using CFRP strips. Two control specimens were prepared to observe the behavior of CFRP strengthened specimens with respect to non-strengthened specimens. The measured 28<sup>th</sup> day average compressive strength of concrete specimens was 28 N/mm<sup>2</sup> with a standard deviation of 3.38 N/mm<sup>2</sup>. The yield strength of steel was 500 N/mm<sup>2</sup> and the nominal cover to the steel reinforcements was 20 mm. The typical reinforcement detail of a sample is shown in Fig. 1 and the flexural reinforcement ratio provided at the bottom of slab was 0.0055.

### 2.2. Specimen preparation and testing

A total of eight slab-column connections were externally strengthened using CFRP with four different arrangements. The test series was prepared such that the strengthened specimens fall into two main categories depending on the CFRP arrangement on the tension face; orthogonally attached CFRP strips and skewed attached CFRP strips. Each of the above categories contained two sub categories depending on the anchorage provided to the external CFRP strips at both ends (Fig. 2). The notations for specimens used in the experimental series are listed in Table 1. The effect from the arrangements of CFRP strips and the effect from end anchorage to the externally bonded CFRP systems were observed using the strengthening schemes shown in Fig. 2. Each strengthening arrangement consisted of four 1 mm × 100 mm × 700 mm CFRP plates attached onto the tension face at 75 mm (the effective depth of the slab) away from the column face. End anchorages were provided at the two ends of each CFRP plate strip using two 10 mm diameter steel bolts connected to a steel plate of 150 mm × 50 mm. CFRP was attached on the grinded concrete surface at the tension face using two-part epoxy adhesive [14].

Specimens were supported on steel I sections and the load was applied through the middle stub column. The flange width of the I beam was 100 mm. The corners of the slab were free to lift. A slight uplift of corners was observed during testing. However, it was negligible with respect to the central deflection. A steel cap with a rubber bottom was used on the column stub to distribute the load monolithically to the top of the column ensuring the column would not fail prior to the slab. Test setup instrumentation was done as in Fig. 3 and point load was applied on the stub column monolithically at a rate of 5 kN/min until the failure of each specimen. Mid span deflection corresponding to the applied load was measured. Crack propagation at the tension surface of the specimens was examined throughout the loading procedure. Failure loads and

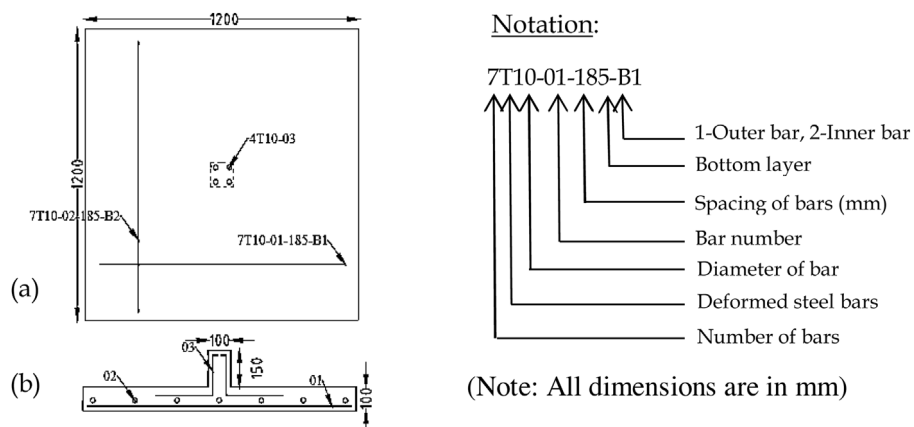


Fig. 1. Reinforcement Details, (a) Plan, (b) Sectional elevation.

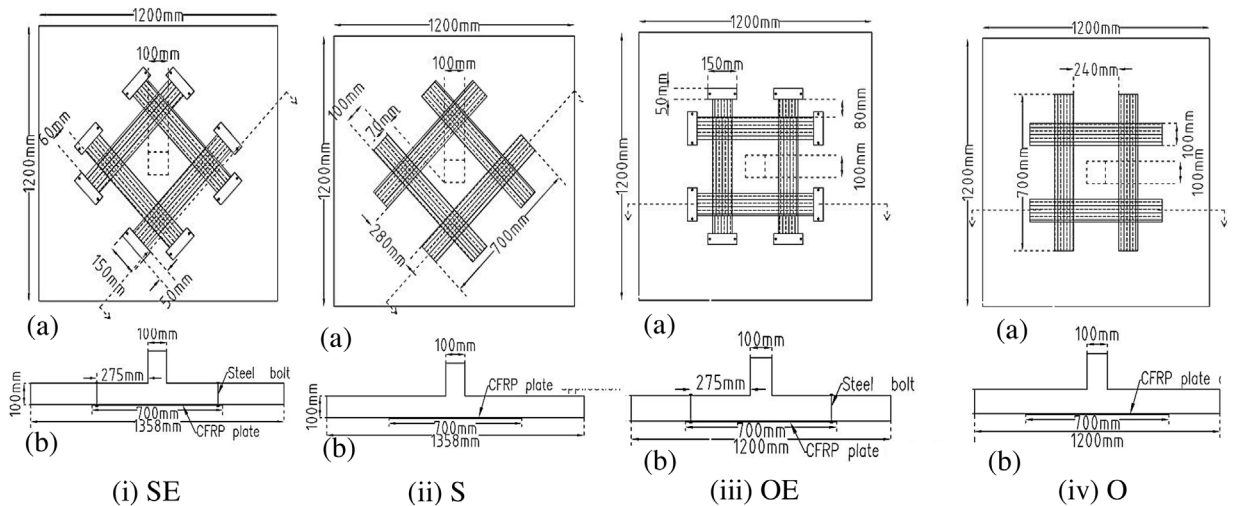


Fig. 2. Strengthening schemes; (i) SE (ii) S (iii) O (iv) OE.

**Table 1**  
Strengthening Scheme.

Specimen Notation	Description	Number of specimens
<b>C</b>	Non-strengthened specimens	2
<b>SE</b>	CFRP attached on tension face in skewed direction with end anchorage	2
<b>S</b>	CFRP attached on tension face in skewed direction without end anchorage	2
<b>OE</b>	CFRP attached on tension face in orthogonal direction with end anchorage	2
<b>O</b>	CFRP attached on tension face in orthogonal direction without end anchorage	2

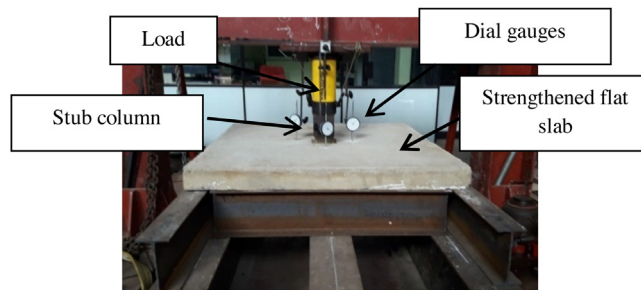


Fig. 3. Test set up and instrumentation.

initial cracking loads were recorded. The average strength enhancement and deflections noted during testing are shown in Table 2.

### 3. Finite element modeling

A three dimensional (3D) finite element model was developed to predict the behavior of CFRP strengthened flat slab-column connections. A commercially available finite element software ABAQUS [15] was used to develop the model. By considering the symmetry of a panel, one-quarter of each specimen was modeled with relevant boundary conditions as shown in Fig. 4 [16]. The symmetric planes were restrained in their perpendicular directions. In the experiment, the bottom of each I beam was fixed to the floor and therefore, in the numerical study the boundary condition was provided as fixed. The contact region at the top flange of I beam and the bottom part of the slab was restrained in the vertical direction using constraints in the FEM analysis (Fig. 4). The analysis type performed was quasi-static ABAQUS/Explicit because it performs faster than ABAQUS/Standard. Though it uses dynamic solution procedures for calculations, under slow loading rates it gives approximate static solutions [16]. Further, it has been assumed that, the actual load applied to the column transfers the load

**Table 2**  
Test Results.

Specimen	Ultimate load (kN)	Maximum deflection (mm)	Load capacity Increment (%)	Specimen	Ultimate load (kN)	Maximum deflection (mm)	Load capacity Increment (%)
<b>C-a</b>	103	13.8	–	<b>C-b</b>	98.64	9.77	–
<b>SE-a</b>	147.15	10.125	46.0	<b>SE-b</b>	147.15	12.08	46.0
<b>S-a</b>	103.00	8.88	2.2	<b>S-b</b>	122.60	13.00	21.6
<b>OE-a</b>	137.34	14.00	36.2	<b>OE-b</b>	127.53	12.08	26.5
<b>O-a</b>	137.34	11.60	36.2	<b>O-b</b>	122.63	10.69	21.6

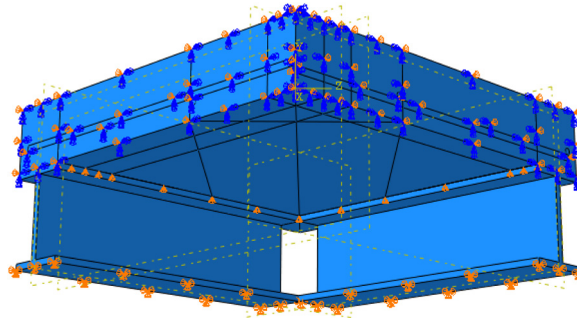


**Fig. 4.** Boundary conditions.

evenly as a pressure onto the slab area where the column was situated. The loading rate used for the pseudo-static analysis in ABAQUS was 5 kN/min. Measured material properties of CFRP and epoxy adhesive used for the model are listed in Table 3.

The model contains four materials; concrete, CFRP, adhesive and, steel reinforcements. Modeling of concrete and steel was done using 3D solid continuum 6-node linear triangular prism elements with reduced integration (C3D6R). The purpose of developing reduced integration elements was to increase computational efficiency with a minimum loss of accuracy. The damage simulation of concrete was done using Concrete Damage Plasticity Model (CDPM), which is capable of representing the damage characteristics as well as the complete inelastic behavior of concrete both in tension and compression. The damage properties are listed in Table 4. A mesh sensitivity analysis was conducted for concrete in the range 10 mm × 10 mm and 25 mm × 25 mm and based on that, the mesh density 20 mm × 20 mm yielded optimum solutions as the maximum aggregate size used in the experiment was 20 mm. Since the failure of each slab-column connection was governed by concrete, the damage properties of steel have not been introduced in the model. Steel only yielded during the experiment and therefore, only elastic and plastic properties were introduced to the program. The steel elements were embedded in the concrete elements, assuming a perfect bond between two materials [7]. The mesh size of 5 mm was introduced for steel. The complete meshed model is shown in Fig. 5.

In order to reduce the computational time, one-quarter of the specimen was modeled. The deflection variation obtained from the finite element analysis is shown in Fig. 6 using coloured contours. The maximum deflection was observed at the center of the slab. During the experiment, an uplift from the edges of the specimens was noted and this was observed in the finite element analysis as well. The Fig. 6(b) shows the positive deflections in colored contours to represent the uplift at edges. The contours have been defined in short intervals as the uplift area deflection change was not visible when the deflection contour interval was wide.

CFRP was modeled using 6-node triangular in-plane shell elements (SC6R) and the adhesive layer was modeled using 6-node three-dimensional cohesive element (COH3D6). The failure of an adhesive bonded CFRP composite material should be designed to fail either in the CFRP sheet material or bonding material or both [17,18]. Therefore, modeling of proper damage properties of CFRP materials and adhesives is crucial in numerical modeling. Since unidirectional CFRP behavior is elastic-

**Table 3**  
Measured material properties.

Property	Epoxy	CFRP
Tensile Strength (MPa)	45	4000
Modulus of Elasticity (MPa)	579	240000
Ultimate Strain	0.043	0.002
Poisson's ratio	0.3	0.3

**Table 4**  
Damage properties of concrete.

Dilation Angle	Eccentricity	$f_{bd}/f_{c0}$	K	Viscosity Parameter
45	0.1	1.16	0.667	0.001

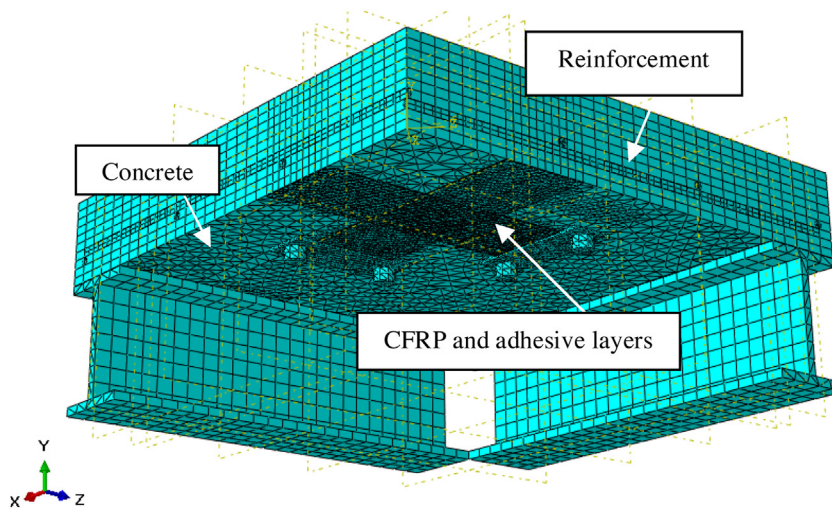


**Fig. 5.** Meshed model; one quarter of the specimen.

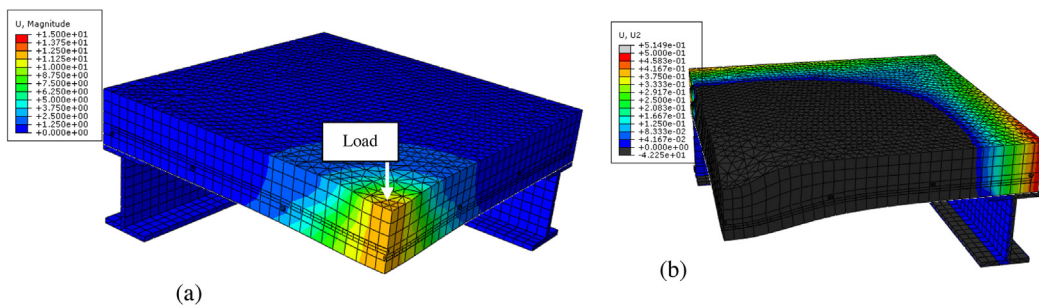


**Fig. 6.** Deflection contours (a) 3D view of model-deflection contours from 0 mm to 15 mm (b) the uplift at the edges.

**Table 5**  
Experiment results and finite element modeling results.

Specimen	Experiment Results		Finite Element Modeling Results		$U_{FEM}$ variation w.r.t. $U_{exp}$	$\delta_{FEM}$ variation w.r.t. $\delta_{exp}$
	Ultimate Load ( $U_{exp}$ )	Ultimate Deflection ( $\delta_{exp}$ )	Ultimate Load ( $U_{FEM}$ )	Ultimate Deflection ( $\delta_{FEM}$ )		
O	130 kN	11.2 mm	140 kN	12.9 mm	1.08	1.15
OE	132 kN	13.0 mm	153 kN	17.9 mm	1.16	1.37
S	113 kN	10.9 mm	111.5 kN	11.0 mm	0.99	1.01
SE	147 kN	11.1 mm	166 kN	12.6 mm	1.13	1.14

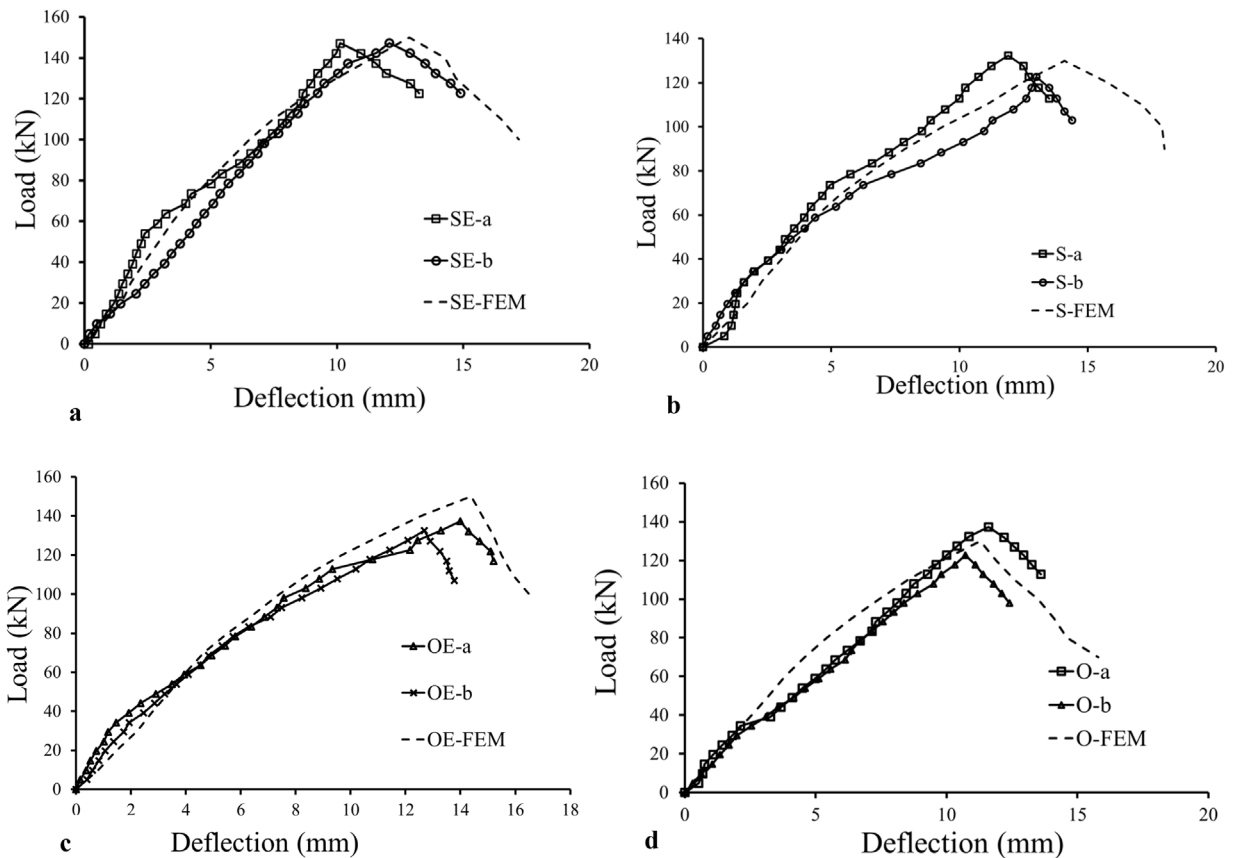


**Fig. 7.** Load-deflection curves (a) skewed end anchored CFRP (b) skewed non-end anchored CFRP (c) orthogonal end anchored CFRP and (d) orthogonal non-end anchored CFRP.

brittle [19], the damage initiation was done based on Hashin's damage criteria taking account for the failure modes of fiber in tension and fiber in compression [17].

The modeling of the adhesive layer is important to predict both onset and propagation of delamination. The adhesive layer was modeled as a cohesive zone using the continuum approach. The cohesive layer thickness was taken as 0.1 mm. Adjacent material components; adhesive and CFRP sheets were attached using tie constraints assuming a perfect bond and the interface between the concrete and the adhesive was modeled by defining interaction properties based on the tangential slip behavior.

### 3.1. Finite element model results comparison with experimental results

Load versus deflection, ultimate strength and crack propagation were used for the validation of numerical model developed in ABAQUS. The ultimate load and the deflection observed both experimentally and numerically are listed in Table 5 and the load versus deflection behaviors of the specimens are shown in Fig. 7. It clearly shows that by means of a suitable external strengthening method, the punching shear capacity could be increased.

A similar deflection increment behavior was observed during the experiment from all tested specimens till they reach 30 kN load (20% of the ultimate load). Similar behavior was noted in recent literature as well [15]. The specimens in which the CFRP strips were attached in skewed direction with end anchors had shown the lowest deflection increment rate with the highest load carrying capacity of 46% with respect to the control specimens. Further, the attaching of CFRP in skewed direction and the introduction of end anchorages onto the CFRP strips had caused for the reduction in deflection increment rate. These samples had clearly indicated the transition of punching shear failure mode to flexural failure mode with external strengthening using CFRP. This implies that the enhanced punching shear capacity was more than 12% to 46% during testing because the dominant failure mode was the flexural failure.

In the experiment, the control specimens were tested to identify the mode of failure, ultimate load carrying capacity and deflection at failure. The conical stress distribution through a slab section due to the point load from the column cannot be observed during the experiment and therefore the finite element analysis was used to observe the stress initiation and propagation as shown in Fig. 9. Although the CDPM does not have the notion of cracks developing at the

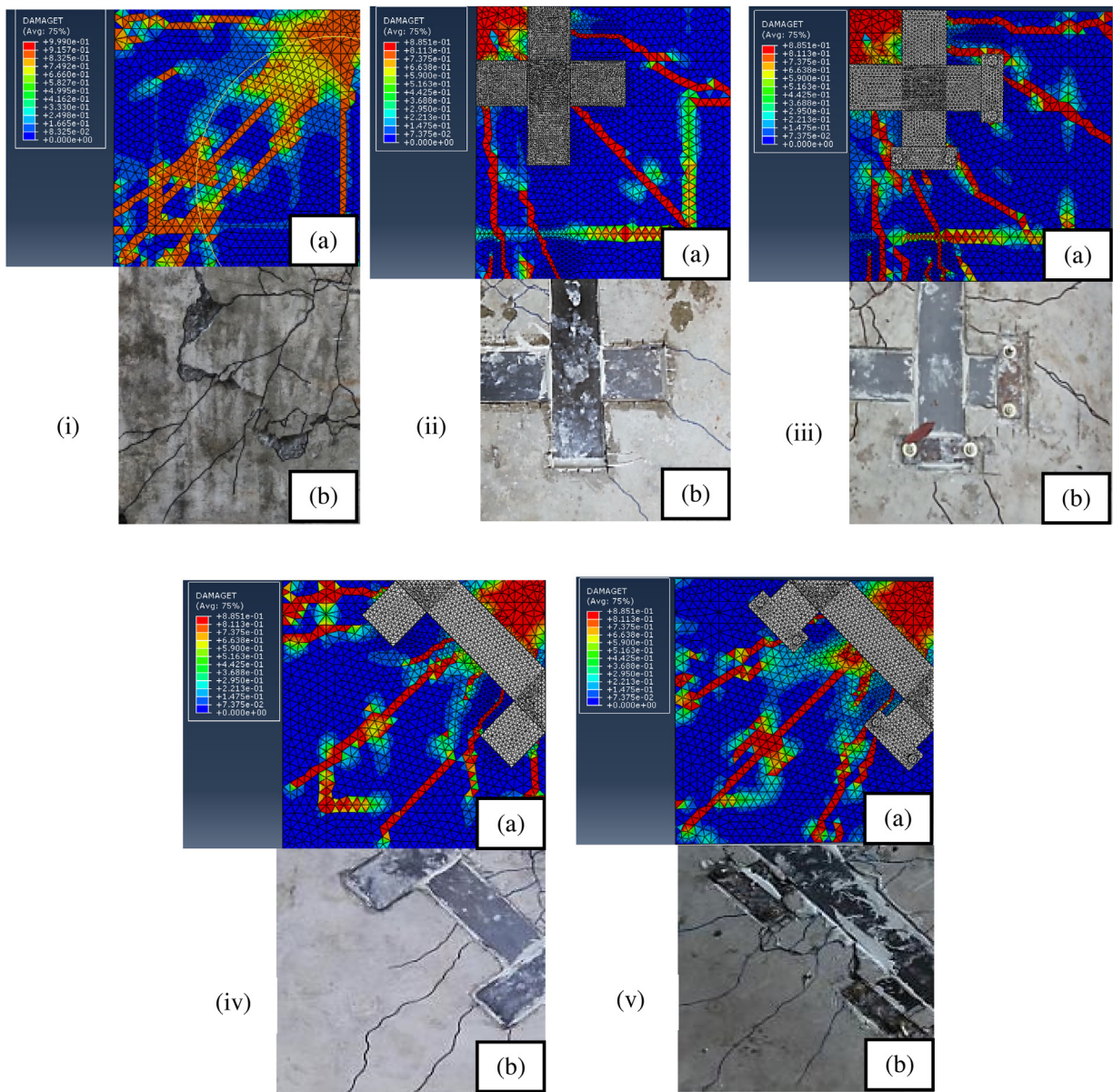


**Fig. 8.** Comparison of crack patterns (i) Control panel (ii) orthogonal non-end anchored CFRP (iii) orthogonal end anchored CFRP (iv) skewed non-end anchored CFRP and (v) skewed end anchored CFRP.

material integration point, it is possible to indicate the effective crack direction with the aid of graphical visualization as indicated in Fig. 8. According to Fig. 8(i), in the non-strengthened control specimen, the punching shear crack was formed at a distance of 3 to 5 times the effective depth away from the column face. This indicates both experimentally and numerically that the punching shear critical perimeter laid 1.5 to 2.5 times the effective depth away from the column surface. The first flexural crack at the tension face of control sample was initiated at 50 kN load level. Then the flexural cracks started propagating in the radial direction starting from the center of the slab. The sudden failure occurred followed by a wide punching shear crack.

The CFRP externally attached specimens; S, SE, O and OE specimens were failed in flexural failure mode indicating average crack widths of 1 mm. The experimental failure loads of these strengthened specimens were identified after the sudden load drop shown at the hydraulic jack. During the experiment, debonding was observed at the edges of the CFRP strips in the S and O type specimens because of the absence of end anchorage at ends. According to the stress behavior shown in the finite element analysis, the adhesive/concrete interface had debonded at strip edge areas during the failure (Fig. 10(a)). Either experimentally or numerically, CFRP strips showed no rupture due to the high tensile strength. Further, the stresses at the adhesive/concrete interface were much lower compared to CFRP end-anchored specimens because the

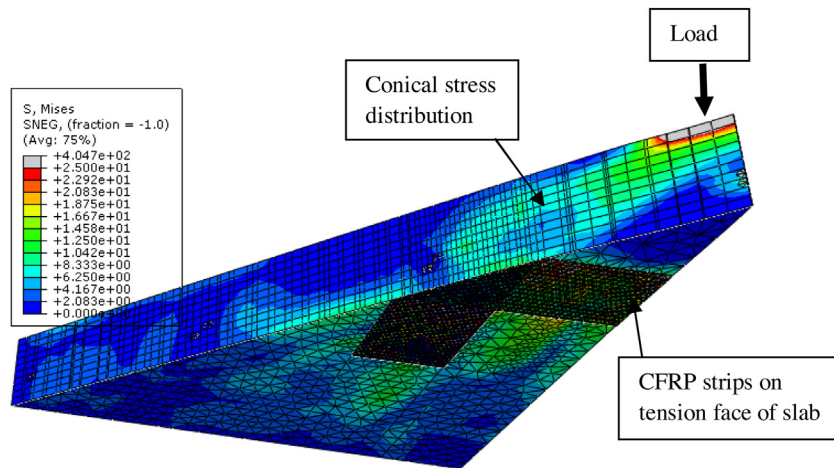


Fig. 9. Conical stress distribution through the slab.

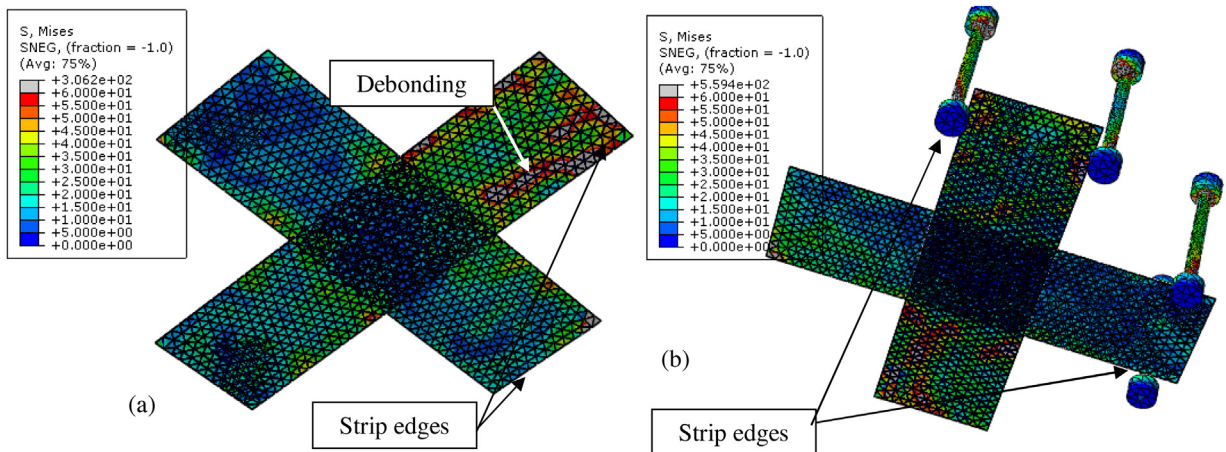


Fig. 10. Stress distribution at the concrete/adhesive interface (a) non-end anchored specimen (b) end anchored specimen.

steel bolts had transferred the developed stress at tension face through the slab section and it is clearly indicated in Fig. 10(b).

#### 4. Conclusions

The numerical and experimental studies were conducted to determine the performance of the external strengthening of slab-column connections with CFRP near the column face to enhance the punching shear performance. The following conclusions were made:

- Eight flat slab-column specimens were strengthened externally with alternative CFRP arrangements and another two specimens were kept as control samples. The results indicated that the skewed placement of CFRP at the shear critical area is effective than that of orthogonal placement in the presence of end anchorage. More than 46% of punching shear capacity can be gained by the external strengthening of slab-column connections with a proper bond arrangement.
- The punching shear critical perimeter in control panel lies between 1.5 to 2.5 times the effective depths away from the column face and it indicates that the Eurocode 2 punching shear critical perimeter predictions is valid.
- Irrespective of the CFRP arrangement at the tension face of specimens, the provision of end anchorage to CFRP strips increases the load carrying capacity.
- Debonding of CFRP strips was noticed at the failure of non-end anchored specimens during the experiment. Further, the FEM from ABAQUS/Explicit predicted the stress critical areas at the concrete/adhesive interface which could lead to debonding.



- Limitations of the FEM could effect the outcomes of the numerical modelling described in this study. Such limitations are; the mesh sensitivity of the model, measured material property accuracy level fed to the numerical model, limitations to validate the numerical model with the experimental model, etc.

## 5. Data availability

The raw/processed data required to reproduce these findings cannot be shared at this time as the data also forms part of an ongoing study.

## Declaration of Competing Interest

None.

## Acknowledgments

This work would not have been possible without the financial support provided by the SRC grant No: SRC/LT/2017/23 from the University of Moratuwa, Sri Lanka. The authors would like to extend their gratitude to the Airow Solutions (Pvt) Ltd, Maharagama, Sri Lanka, for providing materials for this study.

## References

- [1] P. Behzard, M.K. Sharbatdar, A. Kheyroddin, Different NSM FRP technique for strengthening of RC two-way slabs with low clear cover thickness, *Sci. Iran.* 23 (2) (2016) 520–534, doi:<http://dx.doi.org/10.24200/sci.2016.2136>.
- [2] M.L.V.P. Malalanayake, J.C.P.H. Gamage, M.A.L. Silva, Experimental investigation on enhancing punching shear capacity of flat slabs using CFRP, 8th International Conference on Structural Engineering and Construction Management (ICSECM2017), Kandy, Sri Lanka, 2017.
- [3] M.R. Esfahani, M.R. Kianoush, A.R. Moradi, Punching shear strength of interior slab–column connections strengthened with carbon fiber reinforced polymer sheets, *Eng. Struct.* 31 (7) (2009) 1535–1542, doi:<http://dx.doi.org/10.1016/j.engstruct.2009.02.021>.
- [4] E.H. Rochdi, D. Bigaud, E. Ferrier, P. Hamelin, Ultimate behavior of CFRP strengthened RC flat slabs under a centrally applied load, *Compos. Struct.* 72 (1) (2006) 69–78, doi:<http://dx.doi.org/10.1016/j.compstruct.2004.10.017>.
- [5] Luca Tassinari, Miguel Fernández Ruiz, Aurelio Muttoni, Sagasetta Juan, Non-axis-symmetrical punching shear around internal columns of RC slabs without transverse reinforcement, *Mag. Concr. Res.* 63 (2011) 441–457, doi:<http://dx.doi.org/10.1680/macr.10.00098>.
- [6] R.H.M. Dissanayaka, M.A.L. Silva, L.P.G. Magallagoda, J.C.P.H. Gamage, Physical behavior of CFRP retrofitted reinforced concrete slab–column connections, 9th International Conference on Sustainable Built Environment (ICSBE2018), Kandy, Sri Lanka, 2018.
- [7] M.A.L. Silva, W.I. Madushanka, P.S.I. Ariyasena, J.C.P.H. Gamage, Punching shear capacity enhancement of flat slabs using end anchored externally bonded CFRP, *Soc. Struct. Eng. Sri Lanka MODULUS* 28 (2) (2018).
- [8] S.T. Smith, H. Zhang, Z. Wang, Influence of FRP anchors on the strength and ductility of FRP-strengthened RC slabs, *Constr. Build. Mater.* 49 (2013) 998–1012, doi:<http://dx.doi.org/10.1016/j.conbuildmat.2013.02.006>.
- [9] R. Kalfat, Anchorage Systems in Concrete Structures Strengthened with Carbon Fiber Reinforced Polymer, Department of Engineering and Industrial Sciences Swinburne University of Technology, 2014.
- [10] M.H. Miami, D. Mostofinejad, H. Nakamura, Strengthening of flat slabs with FRP fan for punching shear, *Compos. Struct.* (2014), doi:<http://dx.doi.org/10.1016/j.compstruct.2014.08.041>.
- [11] M.H. Meisami, D. Mostofinejad, H. Nakamura, Strengthening of flat slabs with FRP fan for punching shear, *Compos. Struct.* 119 (2014) 305–314, doi:<http://dx.doi.org/10.1016/j.compstruct.2014.08.041>.
- [12] J. Einpaul, F. Brantschen, M. Fernández Ruiz, A. Muttoni, Performance of punching shear reinforcement under gravity loading: influence of type and detailing, *ACI Struct. J.* 113 (4) (2016) 827–838, doi:<http://dx.doi.org/10.14359/51688630>.
- [13] M.R. Esfahani, M.R. Kianoush, A.R. Moradi, Punching shear strength of interior slab–column connections strengthened with carbon fiber reinforced polymer sheets, *Eng. Struct.* 31 (7) (2009) 1535–1542, doi:<http://dx.doi.org/10.1016/j.engstruct.2009.02.021>.
- [14] Erandi Ariyachandra, J.C.P.H. Gamage, Riadh Al-Mahaidi, Robin Kalfat, Effects of surface roughness and bond enhancing techniques on flexural performance of CFRP/concrete composites, *Compos. Struct.* (2017), doi:<http://dx.doi.org/10.1016/j.compstruct.2017.07.028>.
- [15] K. Hibbitt, Sorensen, ABAQUS: Theory Manual, Hibbitt, Karlsson & Sorensen, Providence, R.I, 1992.
- [16] A. Genikomso, M. Polak, Finite element analysis of punching shear of concrete slabs using damaged plasticity model in ABAQUS, *Eng. Struct.* 98 (2015), doi:<http://dx.doi.org/10.1016/j.engstruct.2015.04.016>.
- [17] Y.S.S. Al-Kamaki, G.B. Hassan, G. Alsofi, Experimental study of the behaviour of RC corbels strengthened with CFRP sheets, *Case Stud. Constr. Mater.* 9 (2018), doi:<http://dx.doi.org/10.1016/j.cscm.2018.e00181> ISSN 2214-5095.
- [18] K. Soudki, A.K. El-Sayed, T. Vanzwol, Strengthening of concrete slab–column connections using CFRP strips, *J. King Saud Univ. – Eng. Sci.* 24 (1) (2012) 25–33, doi:<http://dx.doi.org/10.1016/j.jksues.2011.07.001>.
- [19] R.Z. Al-Rousan, M.A. Alhassan, E.A. AlShuqari, Behavior of plain concrete beams with DSSF strengthened in flexure with anchored CFRP sheets—effects of DSSF content on the bonding length of CFRP sheets, *Case Stud. Constr. Mater.* 9 (2018), doi:<http://dx.doi.org/10.1016/j.cscm.2018.e00195> ISSN 2214-5095.